



Glutamate 270 plays an essential role in K⁺-activation and domain closure of *Thermus thermophilus* isopropylmalate dehydrogenase

Éva Gráczér^a, Anna Palló^{b,1,2,3}, Julianna Oláh^c, Tamás Szimler^a, Petr V. Konarev^{d,4}, Dmitri I. Svergun^d, Angelo Merli^e, Péter Závodszy^a, Manfred S. Weiss^f, Mária Vas^{a,*}

^aInstitute of Enzymology, Research Centre for Natural Sciences, Hungarian Academy of Sciences, Magyar tudósok krt. 2., H-1117 Budapest, Hungary

^bInstitute of Organic Chemistry, Research Centre for Natural Sciences, Hungarian Academy of Sciences, Magyar tudósok krt. 2., H-1117 Budapest, Hungary

^cDepartment of Inorganic and Analytical Chemistry, Budapest University of Technology and Economics, Gellért Square 4., H-1111 Budapest, Hungary

^dEuropean Molecular Biology Laboratory, Hamburg Outstation, Notkestrasse 85, 22603 Hamburg, Germany

^eUniversità degli Studi di Parma, Dipartimento di Bioscienze, Viale G.P. Usberti 23/A, I-43100 Parma, Italy

^fHelmholtz-Zentrum Berlin für Materialien und Energie, Macromolecular Crystallography (HZB-MX), Albert-Einstein-Str. 15, D-12489 Berlin, Germany

ARTICLE INFO

Article history:

Received 12 November 2014

Revised 1 December 2014

Accepted 2 December 2014

Available online xxxxx

Edited by Peter Brzezinski

Keywords:

Isopropylmalate dehydrogenase

Activation by K⁺

Site-directed mutagenesis

X-ray crystallography

Small angle X-ray scattering

Fluorescence resonance energy transfer

ABSTRACT

The mutant E270A of *Thermus thermophilus* 3-isopropylmalate dehydrogenase exhibits largely reduced (~1%) catalytic activity and negligible activation by K⁺ compared to the wild-type enzyme. A 3–4 kcal/mol increase in the activation energy of the catalysed reaction upon this mutation could also be predicted by QM/MM calculations. In the X-ray structure of the E270A mutant a water molecule was observed to take the place of K⁺. SAXS and FRET experiments revealed the essential role of E270 in stabilisation of the active domain-closed conformation of the enzyme. In addition, E270 seems to position K⁺ into close proximity of the nicotinamide ring of NAD⁺ and the electron-withdrawing effect of K⁺ may help to polarise the aromatic ring in order to aid the hydride-transfer.

© 2014 Published by Elsevier B.V. on behalf of the Federation of European Biochemical Societies.

1. Introduction

3-Isopropylmalate dehydrogenase (IPMDH) belongs to the class of β-hydroxyacid oxidative decarboxylases and catalyses the oxidation and decarboxylation of (2R,3S)-3-isopropylmalate (IPM) to 2-oxo-4-methyl-pentanoate (isocaproic acid) in the presence of NAD⁺ and a divalent cation (Mn²⁺ or Mg²⁺) in the leucine biosynthetic pathway of bacteria [1]. Since the chemical mechanisms of the catalysed reactions are similar, the architecture of the active

sites of this class of enzymes is also very similar [2]. Yet, there are also notable differences in their functional properties, e.g. monovalent cations K⁺ and NH₄⁺ activate IPMDH [3,4] and tartrate dehydrogenase [5], respectively, while isocitrate dehydrogenase is insensitive of their presence [6]. In the crystal structure of the quaternary complex of *Tt*-IPMDH–Mn²⁺–IPM–NADH a bound K⁺-ion was observed in the active site [7]. Among the ligands coordinating K⁺-ion the side-chain of E270 (Fig. 1A) seems to play a peculiar role. This glutamate is a conserved residue throughout in all oxidative decarboxylases, but its exact role in function has not been established, yet. In the present study E270 of *Tt*-IPMDH was replaced by alanine in order to investigate its role in the function and activation of the enzyme by K⁺-ion.

2. Materials and methods

2.1. Enzymes and chemicals

E270 of *Tt*-IPMDH was mutated into Ala using the QuickChange site-directed mutagenesis kit. The modified enzyme was expressed

Abbreviations: IPMDH, 3-isopropylmalate dehydrogenase (EC 1.1.1.85); *Tt*, *Thermus thermophilus*; IPM, (2R,3S)-3-isopropylmalate; MOPS, 3-(N-morpholino)-propane-sulphonic acid; SAXS, small angle X-ray scattering; FRET, fluorescence resonance energy transfer

* Corresponding author.

E-mail address: vas.maria@ttk.mta.hu (M. Vas).

¹ Present address: Structural Biology Research Center, VIB, 1050 Brussels, Belgium.

² Present address: Brussels Center for Redox Biology, 1050 Brussels, Belgium.

³ Present address: Structural Biology Brussels Laboratory, Vrije Universiteit Brussel, 1050 Brussels, Belgium.

⁴ Present address: Laboratory of reflectometry and small-angle scattering, Institute of Crystallography RAS, Leninsky pr. 59, 119333 Moscow, Russia.

<http://dx.doi.org/10.1016/j.febslet.2014.12.005>

0014-5793/© 2014 Published by Elsevier B.V. on behalf of the Federation of European Biochemical Societies.

and purified using the previously published method applied for the wild-type enzyme [8]. The enzyme (about 30 mg/ml) was obtained in a 25 mM MOPS/KOH buffer, pH 7.6 and then lyophilised. 3-Isopropylmalic acid (IPM) was purchased from Wako Biochemicals (Japan), NAD and NADH were Sigma products. All other chemicals were commercially available high purity grade products.

2.2. Crystallisation and X-ray analysis of E270A mutant of Tt-IPMDH

Pure lyophilised mutant (E270A) of Tt-IPMDH was dissolved in distilled water. Crystals were obtained using the hanging drop method at 20 °C by mixing 1 µl protein solution consisting of 20 mg/ml protein, 13 mM MnCl₂, 9 mM IPM and 5 mM NADH with 1 µl reservoir solution consisting of 20% (w/v) PEG 6000, 0.1 M MOPS/KOH pH 7.6, and 10% (v/v) ethanol. The initial concentration of K⁺ in the droplet can be estimated to be about 30 mM. Diffraction data to 2.0 Å resolution were collected from a single crystal on beamline BL14.1 of the Helmholtz-Zentrum Berlin (Germany) [9]. Data were processed using XDS [10] and the structure was determined using MOLREP [11] and the quaternary complex structure of Tt-IPMDH–Mn²⁺–IPM–NADH [7] (PDB entry 4F7I) as a search model. Atomic coordinates were refined using REFMAC5 [12] and manually inspected using COOT [13]. All relevant statistics are presented in Table 1. The refined structure and the corresponding structure factor amplitudes were deposited to the PDB under the accession code 4WUO.

2.3. QM/MM modelling of the redox-reaction catalysed by IPMDH in the absence of the side-chain of E270

In order to ensure maximum comparability with our previous computational results, the Mn²⁺-ion bound generated intermediate structures were taken from that study [7] and the side-chain of the E270 amino acid was mutated in silico to alanine. Bound K⁺-ions were removed and calculations were performed with and without the bound water molecule found in the place of K⁺-ion in the crystal structure of the E270A mutant. In the previous study three different atom-partitioning schemes (QM1-3) were tested [7]. Here we used QM2 of the previous study as the QM region in the calculation. All modelling details were exactly the same as in the previous study. The activation energy of the hydride transfer reaction with and without the bound water molecule was determined using 3–3 QM/MM energy profiles. Final energies published herein were determined at the B3LYP/6–311+G*/MM level of theory.

2.4. Enzyme activity measurements

Activity of IPMDH (wild-type: 6–12 µg/ml, i.e., 0.16–0.32 µM monomer, or E270A mutant: 2.1 mg/ml, i.e., 55 µM) was assayed in the presence of 0.5 mM IPM, 0.5 mM MnCl₂ and 4 mM NAD⁺ in 25 mM MOPS/KOH buffer (pH 7.6). Formation of NADH was recorded spectrophotometrically at 340 nm at 20 °C using a Jasco (Tokyo, Japan) V-550 spectrophotometer equipped with a Grant Y6 thermostat. Alternatively, activities were tested in 25 mM MOPS/NaOH buffer (pH 7.6) at various concentrations of added KCl. The activating effect of K⁺ characterised by its activation (K_A) constant. This value has been determined by fitting the kinetic data using the equation:

$$\frac{V_{\text{act}}}{V_0} = \frac{K_A + V_{\text{max,rel}} \cdot [\text{Me}]}{K_A + [\text{Me}]} \quad (1)$$

where V_0 and V_{act} are velocities of the reaction in the absence and in the presence of the activator, respectively; K_A is the activation constant of metal ion, that numerically equals to the [Me] causing 50% increase of $V_{\text{max,rel}}$; [Me] is the concentration of metal ion;

Table 1
Data collection and processing, structure-refinement and validation statistics.

	4WUO
Data collection	
Wavelength (Å)	0.91841
Crystal to detector distance (mm)	225.0
Rotation range per image (°)	0.2
Total rotation range (°)	128
Data processing	
Space group	C22 ₁
Cell constants (Å)	50.18, 143.25, 174.89
Resolution range	41.6–2.05
Last shell	2.10–2.05
Mosaicity	0.200
Completeness (%)	99.6 (97.9)
No. of observed/unique (last shell)	207793/39957 (14280/2875)
Mean $I/\sigma(I)$	17.23 (2.71)
$R_{\text{r.i.m.}}^a$	0.080 (0.682)
Overall B-factor from Wilson plot (Å ²)	36.1
Optical resolution (Å)	1.64
V_M (Å ³ Da ⁻¹)	1.99
Solvent content (%)	38
Refinement	
No. of reflections, working set	37938 (2716)
No. of reflections, test set	2009 (148)
R_{cryst}	0.170
R_{free}	0.229
DPI(Å)	0.213
Number of atoms	
Protein	5235
Ions	3
IPM	24
NADH	88
Other organic	43
Water molecules	180
R.m.s. deviations	
Bonds (Å)	0.015
Angles (°)	1.7
Average B-factors	
Protein(Å ²)	37.2
Ions	33.4
IPM	28.9
NADH	28.5
Other organic	47.9
Water molecules	36.3
Ramachandran plot	
Most favoured (%)	97.7
Allowed (%)	2.3
No. of dimers/asymmetric unit	1

^a $R_{\text{r.i.m.}} = \left(\frac{\sum (n_i/(n_i - 1))^{0.5} \sum |I_{h_i} - I_{h_j}|}{\sum I_{h_j}} \right)$ with $\langle I_h \rangle = (\sum I_{h_j})/n_j$ [20].

$V_{\text{max,rel}}$ is the maximum relative activation, i.e. the ratio of the maximal activity in the presence and in the absence of the activator.

2.5. FRET measurements

The fluorescence resonance energy transfer (FRET) between Trp(s) of IPMDH and the bound NADH was recorded at 20 °C in the presence of Mg²⁺ and IPM as reported by Dean and Dvorak [14] using a SPEX Fluoromax-3 spectrofluorimeter equipped with a Peltier thermostat (Edison, NJ). The usual mixture contained 12 µg/mL (0.32 µM monomer) IPMDH (wild-type or E270A), 12 µM NADH, 3 mM MgCl₂ and 1 mM IPM. The protein was excited at 295 nm and the emission by the bound NADH was recorded between 300 and 550 nm in a cuvette with 10 mm path length. The slits of 2 and 4 nm were applied for excitation and emission, respectively. All measurements were carried out in the presence of various concentrations of KCl.

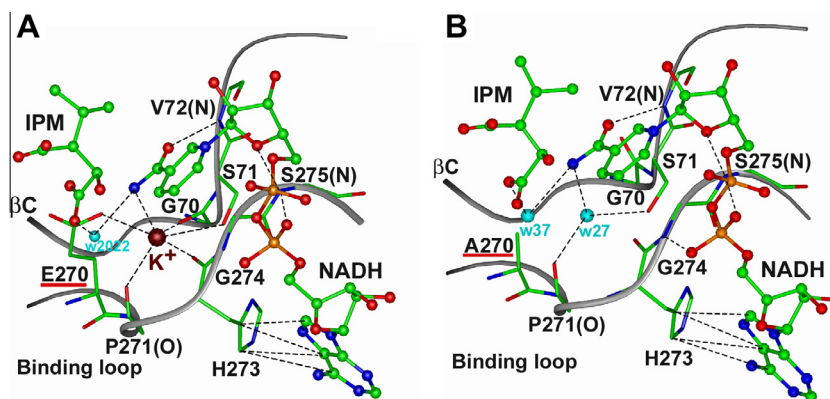


Fig. 1. Structural comparison of the active sites of *Tt*-IPMDH–Mn²⁺–IPM–NADH complexes of the wild-type (A) and the E270A mutant (B). K⁺ is presented with a brown sphere, waters with blue, substrates as ball and stick, and all side-chains coordinating K⁺-ion are shown as stick models coloured according to atom types. Grey ribbons represent part of the β -strand C (residues 66–72) and the nucleotide binding loop (residues 270–277). The dashed lines illustrate atomic distances smaller than 3.5 Å.

2.6. Small angle X-ray scattering (SAXS) measurements and data processing

Synchrotron radiation X-ray scattering data were collected on the P12 beam line at the Hamburg EMBL Outstation (on the PETRA III storage ring, at DESY). Solutions of both wild-type and E270A mutant of *Tt*-IPMDH, their complexes with Mn²⁺, IPM and NADH (non-functioning complex) in 25 mM MOPS/NaOH buffer, pH 7.6, without and with added KCl (cf. Table 3), measured at protein concentrations in the range from 5.0 to 10 mg/ml using pixel 2 M PILATUS detector (DECTRIS, Switzerland) at a sample-detector distance of 3.1 m, and wavelength $\lambda = 1.25$ Å, covering the momentum transfer range $0.01 < s < 0.45$ Å⁻¹ ($s = 4\pi \sin(\theta)/\lambda$ where 2θ is the scattering angle). The concentrations of Mn²⁺, IPM and NADH in the protein samples were 1 mM, 0.5 mM and 5 mM, respectively. To check for radiation damage, twenty 50-ms exposures were compared; no radiation damage effects were observed. The data, after normalisation to the intensity of the incident beam, were averaged, and the scattering of the buffer was subtracted. All data manipulations were performed using the program package PRIMUS [15].

Structural parameters, the forward scattering $I(0)$ and the radius of gyration R_g were evaluated using the Guinier approximation [16] and the program GNOM [17]. The radii of gyration and the scattering patterns from the crystallographic models of wild-type apo *Tt*-IPMDH (pdb: 2Y3Z) and its substrate complex with Mn²⁺, IPM and NADH (pdb: 4F7I) were computed using the program CRY-SOL [18]. The program OLIGOMER [15] was used to calculate the ratio of open- and closed-form species present in *Tt*-IPMDH solutions as described in [19].

3. Results and discussion

3.1. No K⁺-binding is observed in the X-ray structure of E270A mutant

The global structure of E270A mutant IPMDH with bound Mn²⁺, IPM and NADH exhibits a closed conformation, but slightly less closed than that of the previously determined [7] wild-type enzyme. However, the active sites exhibit well defined differences due to the mutation. Fig. 1 illustrates part of the active site of *Tt*-IPMDH with bound IPM and NADH both of the wild-type (A) and the E270A mutant (B) enzymes. In the wild-type enzyme the carboxylate group of E270 is an important electrostatic ligand for K⁺-ion. In the active site of the wild-type IPMDH there was a peak observed on the $F_o - F_c$ difference density map when the K⁺-ion was initially modelled as water, however in case of the E270A mutant enzyme there was no residual density when this peak was modelled as water. Furthermore, chemistry also implies a

different species. In the crystal structure of the wild-type enzyme the partially negatively charged carbonyl of Gly70 coordinates the K⁺-ion, while in the absence of the charged ion, in case of the E270A mutant, the density map shows this carbonyl group facing the other direction (cf. Fig. 1B) and making a water bridged H-bonding interaction (not shown) towards nicotinamide moiety of NADH. Thus, one can assume that E270A mutant lacks the ability of K⁺-binding.

3.2. Activation of IPMDH by K⁺-ion and the kinetic parameters of E270A mutant

Activity of the wild-type *Tt*-IPMDH was tested both in the absence and in the presence of various concentrations of K⁺-ion. Fig. 2A shows the well-pronounced activating effect of K⁺-ion: it increases the k_{cat} value by more than one order of magnitude. Our previous QM/MM calculations, indeed, have shown that the electron-withdrawing effect of K⁺ may polarise the nicotinamide ring of NAD⁺ at its C4-atom and thereby favour the occurrence of the hydride-transfer [7]. On the other hand, the mutant E270A IPMDH, exhibits only a very low (~1%) activity compared to the wild-type enzyme, even in the presence of high excess of K⁺-ion (cf. Fig. 2B). The kinetic parameters of E270A mutant and of the wild-type enzyme are compared in Table 2. Accordingly, E270A exhibits extremely reduced affinity towards K⁺-ion. The activity of E270A is reduced even in the presence of saturating concentration of K⁺-ion, suggesting that the glutamate side-chain of E270 itself has some additional catalytic role. The crystal structure shows that E270 is in a direct interaction with the nicotinamide group (cf. Fig. 1A) and thereby contributes to its proper orientation for the reaction. Indeed, the K_m -value of NAD⁺ is increased significantly for E270A compared to that of the wild-type enzyme (Table 2). Furthermore, as it will be shown below, the side-chain of E270 may stabilise the active closed conformation of the enzyme.

3.3. Estimated activation energy of the redox step of IPMDH catalysed reaction in case of E270A mutant

In order to estimate the activation energy of the hydride transfer reaction, 3–3 parallel QM/MM energy profile calculations were carried out for the E270A mutant enzyme with and without the bound water molecule present in the place of K⁺-ion. The presence of the water molecule had no significant influence on the obtained activation energies. In the case of the three profiles the activation energies in the mutant increased to 18.4, 21.1 and 22.2 kcal/mol, which corresponds to an increase of 3.5, 4.6 and 3.9 kcal/mol,

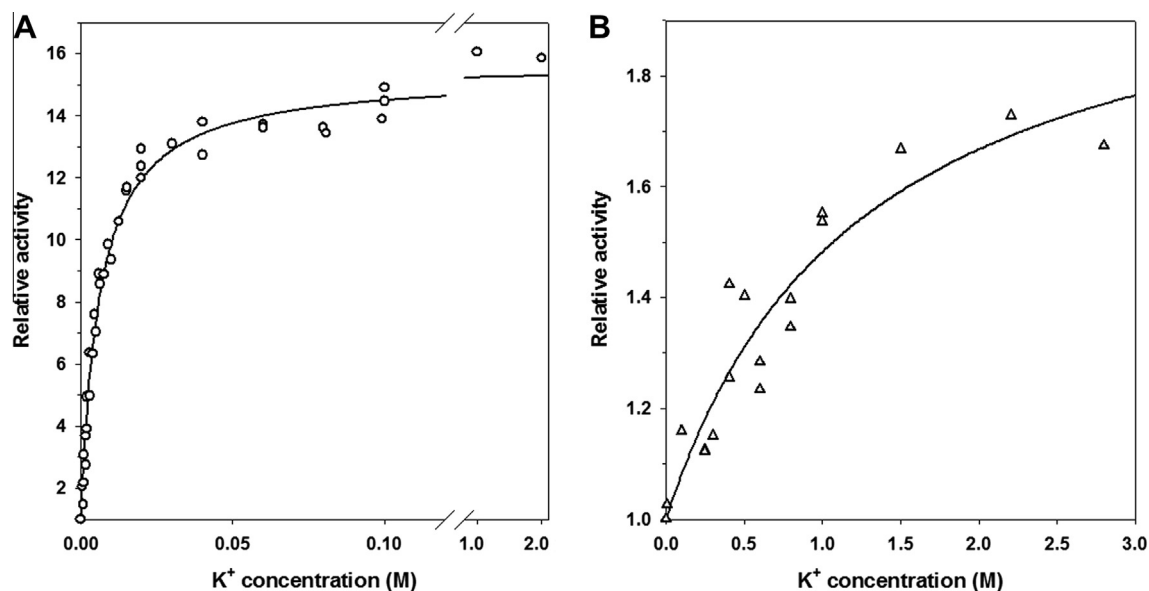


Fig. 2. Activation of IPMDH by K^+ -ion. For measuring the activities of wild-type (o-o) (A) and E270A mutant (Δ - Δ) (B) IPMDHs the substrates were applied at closely saturating concentrations (cf. Methods) and the concentration of K^+ -ion was varied. The activities (relative to the one in the absence of K^+ -ion) are plotted against K^+ -concentration. The activating constants of K^+ -ion have been determined by fitting the continuous lines to the experimental data using Eq. (1) and summarised in Table 2.

Table 2
Kinetic constants of E270A mutant in comparison to the wild-type *Tt*-IPMDH. The kinetic measurements have been carried out as described in the Section 2 under the conditions specified in the legends to Fig. 2.

Kinetic constants		Wild-type	E270A mutant
k_{cat} (min^{-1})	No K^+	15.3 ± 4	0.95 ± 0.2
	Saturating [K^+]	238 ± 30^b	1.96 ± 0.3
K^+ -ion K_A^a (mM)	Varying concentrations of K^+	6.1 ± 0.6	1240 ± 200
	25 mM K^+	16 ± 3^b	32 ± 5
NAD K_m (μM)		290 ± 50	660 ± 55
Mn^{2+} K_m (μM)		10 ± 4^b	25 ± 6

^a K_A^a : activatory constant.

^b These kinetic constants has been determined earlier [19].

respectively, compared to the wild-type, K^+ -bound structure [7]. Based on chemical thermodynamics it can be expected that 3–4 kcal/mol increase in the activation energy decreases the reaction rate 150–1000 fold, which is the range for the experimentally

observed 242-fold decrease in the k_{cat} value of the mutant enzyme in the absence of K^+ compared to the wild-type enzyme at saturating K^+ -ion concentration.

3.4. Both K^+ -ion and the side-chain E270 are essential for FRET-formation

It has been noted that spectral changes, characteristic of FRET from the Trp side-chain(s) of IPMDH to the bound NADH can occur but, interestingly only if the substrate IPM is also bound and stabilises the closed (active) conformational state of the enzyme [14]. On this basis FRET phenomenon of IPMDH is assumed to be a characteristics of its domain-closed conformation. Here we found that even in the presence of bound K^+ -ion the mutant E270A exhibits a FRET spectrum with small intensity compared to the well-formed high intensity spectrum of the wild-type enzyme. In addition, the K^+ -free enzymes (either wild type or E270 mutant) exhibit only very negligible FRET spectra (Fig. 3A). These results raise the possibility of prevention of domain closure upon either mutation of E270 or in the absence of bound K^+ -ion. The large spectral changes

Table 3
Comparison of SAXS experimental data with those derived from the crystallographic models.

SAXS experiments	R_g , Å ^a		Discrepancy values χ between the scattering from crystallographic models and experimental data			Volume fractions of open/closed structures	
	GNOM method	Guinier method	Closed crystal structure	Open crystal structure	Open/closed mixture ^c	V_{closed} , %	V_{open} , %
<i>Tt</i> -IPMDH–Mn–IPM–NADH							
Wild-type (no K^+)	27.4 ± 0.2	27.4 ± 0.3	1.18	1.19	1.09	53 ± 3	47 ± 3
Wild-type (50 mM K^+)	27.2 ± 0.2	27.3 ± 0.3	1.17	1.20	1.11	58 ± 3	42 ± 3
E270A mutant (no K^+)	28.3 ± 0.2	28.4 ± 0.3	2.03	1.15	1.14	4 ± 3	97 ± 5
E270A mutant (1 M K^+)	28.4 ± 0.2	28.5 ± 0.3	1.71	1.08	1.07	5 ± 3	95 ± 5
R_g (theoretical), angstroms ^b			26.67	28.45			
Molecular mass, kDa ^b			74.3	73.8			

The minimum values of discrepancy (in bold) indicate the best correlation between SAXS data and crystallographic model.

The small variations in the calculated molecular mass are due to different numbers of residues resolved in different crystal structures.

^a The R_g values were computed by two alternative methods, using the program GNOM and Guinier approximation, respectively.

^b Radius of gyration and molecular mass of the high resolution models as retrieved from the PDB: 4F71 for the closed crystal structure of the quaternary complex of *Tt*-IPMDH–Mn–IPM–NADH and 2Y3Z for the open crystal structure of apo *Tt*-IPMDH.

^c The fits for open/closed mixture were obtained by OLIGOMER, V_{open} and V_{closed} correspond to the volume fractions of each state found by OLIGOMER.

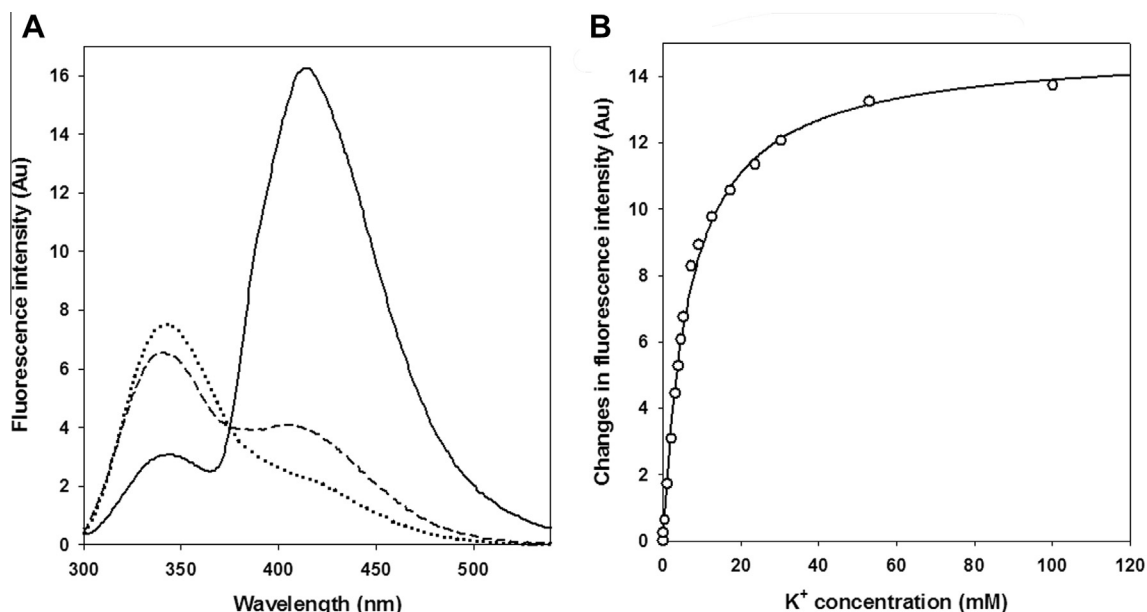


Fig. 3. Effect of E270A mutation and the K^+ -ion on the FRET spectrum of IPMDH. (A) Fluorescence emission spectra of FRET (cf. Methods) characteristic of the wild-type IPMDH is recorded in the absence (dotted line) and in the presence of 100 mM K^+ -ion (continuous line). The measurement has been repeated with the mutant E270A in the presence of 500 mM KCl (dashed line). It is noted that in the absence of K^+ -ion the spectrum of the E270A mutant coincides with that of the wild-type enzyme (dotted line), indicating formation of very negligible FRET spectra in both cases. (B) Titration of the wild-type IPMDH (0.32 μ M) with K^+ -ion by the aid of the FRET signal at $\lambda_{\text{emission}} = 410$ nm.

observed upon addition of K^+ -ion to the wild-type enzyme allowed us to determine its binding constant (Fig. 3B) that is found to be $K_d = 5.0 \pm 0.6$ mM, i.e. in good agreement with the value of the activatory constant (K_A) determined above (Table 1). However, to test the effects of mutation (E270A) or removal of K^+ -ion on the domain opening/closing requires more direct experiments. Therefore, SAXS-experiments have been devised.

3.5. Domain closure is prevented upon mutation of E270A

SAXS is the most appropriate method to test protein conformational changes occurring in solution, especially if it is accompanied by changes in the shape of the molecule, such as the domain closure.

In our previous studies with the wild-type *Tt*-IPMDH we clearly detected domain closure in the complex with Mn^{2+} and IPM [19]. This experiment was repeated with the mutant E270A that also binds the substrate Mn -IPM. Table 3 summarises the calculated R_g values and the extent of domain closure as expressed by percentage of the open and closed forms estimated as described in the Methods. The results show that in solution E270A retains its open conformation even in the quaternary Mn -IPM-NADH-IPMDH complex, both in the presence and in the absence of K^+ -ion. Thus, in the absence of this glutamate side-chain the tertiary interactions stabilising the enzyme-closed conformation are possibly weakened. Indeed, the electrostatic interactions of the carboxylate of E270 with the side-chains of R94 and R104 that would stabilise the closed state of Hinge 1 (cf. Fig. 4) are absent in the structure of E270A mutant. Thus, the low activity of the mutant is not only due to the weak interactions with K^+ (cf. Table 2), but also to the predominance of the open conformation, and perhaps to the slow equilibration between the open-closed forms. It may also be noted that during the long time of crystal growing the closed conformation can be selected and the open-closed conformational equilibrium can be shifted towards this less soluble form.

The effect of K^+ -ion on the domain closure was also investigated and, in contrast to the expectation, no significant effect was

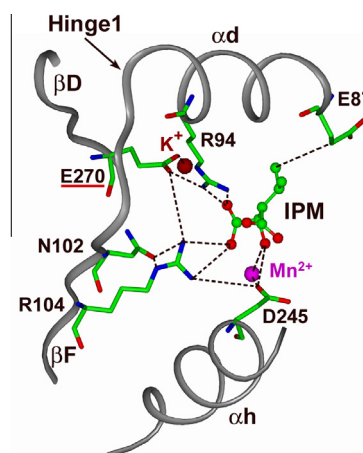


Fig. 4. Effect of E270 side-chain on the conformation of Hinge 1 of IPMDH. Constituents of Hinge 1 including α -helix d and β -strand F as well as its surroundings including the IPM and K^+ -binding sites are represented by grey ribbon diagrams. The substrate IPM (ball and stick model) and the interaction side-chains (stick models) are coloured according to atom types. K^+ - and Mg^{2+} -ions are represented by brown and violet spheres, respectively.

detected (Table 3). Thus, domain-closed conformation for the wild-type enzyme can be formed even in the absence of K^+ -ion, i.e. in the absence of formation of the FRET spectrum (Fig. 3A). It follows, therefore, that appearance of the FRET spectrum is not always an indication of the domain closed conformation, as was assumed previously. The bound K^+ -ion may itself contribute to the occurrence of FRET by sensitively influencing the plane orientation of the quinoidal-ring of the bound NADH.

4. Conclusions

A conserved glutamate side-chain (E270) in the active site of *Tt*-IPMDH exhibits multiple roles: (i) it is the main coordinating

ligand of the activation potassium ion; (ii) it orients properly the reacting nicotinamide ring of NAD⁺ optimal for the enzymatic reduction and (iii) it contributes to the formation of the active, closed conformation. This glutamate is conserved among the oxidative decarboxylases and its direct and/or indirect effects may be generalised.

Acknowledgements

The financial support by the grants OTKA – Hungary (NK 108642) of the Hungarian National Research Fund is gratefully acknowledged. We are also grateful to the EMBL-HH (Hamburg Outstation, Germany) and HZB (Berlin) for access to their synchrotron facilities. The research leading to these results has received funding from the European Community's Seventh Framework Programme (FP7/2007–2013) under grant agreement No. 226716. D.I.S. and P.V.K. acknowledge support from the German Ministry of Education and Science (BMBF) project BIOSCAT, Grant 05K20912. A.P. gratefully acknowledges the support of M. Czugler (Research Centre for Natural Sciences, Hungarian Academy of Sciences, Budapest, Hungary) and thanks the National Science and Technology Office (Hungary) for an X-ray diffractometer purchase grant (MU-00338/2003). J.O. acknowledges the support of the János Bolyai Research Scholarship of the Hungarian Academy of Sciences.

References

- [1] Hayashi-Iwasaki, Y. and Oshima, T. (2000) Purification and characterization of recombinant 3-isopropylmalate dehydrogenases from *Thermus thermophilus* and other microorganisms. *Methods Enzymol.* 324, 301–322.
- [2] Aktas, D.F. and Cook, P.F. (2009) A lysine-tyrosine pair carries out acid-base chemistry in the metal ion-dependent pyridine dinucleotide-linked beta-hydroxyacid oxidative decarboxylases. *Biochemistry* 48, 3565–3577.
- [3] Sekiguchi, T., Harada, Y., Shishido, K. and Nosoh, Y. (1984) Cloning of beta-isopropylmalate dehydrogenase gene from *Bacillus coagulans* in *Escherichia coli* and purification and properties of the enzyme. *Biochim. Biophys. Acta* 788, 267–273.
- [4] Yamada, T., Akutsu, N., Miyazaki, K., Kakinuma, K., Yoshida, M. and Oshima, T. (1990) Purification, catalytic properties, and thermal stability of threo-Ds-3-isopropylmalate dehydrogenase coded by *leuB* gene from an extreme thermophile, *Thermus thermophilus* strain HB8. *J. Biochem. (Tokyo)* 108, 449–456.
- [5] Serfozo, P. and Tipton, P.A. (1995) Substrate determinants of the course of tartrate dehydrogenase-catalyzed reactions. *Biochemistry* 34, 7517–7524.
- [6] Miller, S.P., Goncalves, S., Matias, P.M. and Dean, A.M. (2014) Evolution of a transition state: role of lys100 in the active site of isocitrate dehydrogenase. *ChemBioChem* 15, 1145–1153.
- [7] Palló, A., Oláh, J., Gráczer, E., Merli, A., Závodszy, P., Weiss, M.S. and Vas, M. (2014) Structural and energetic basis of isopropylmalate dehydrogenase enzyme catalysis. *FEBS J.* 281, 5063–5076.
- [8] Gráczer, É., Varga, A., Melnik, B., Semisotnov, G., Závodszy, P. and Vas, M. (2010) Symmetrical refolding of protein domains and subunits: example of the dimeric two-domain 3-isopropylmalate dehydrogenases. *Biochemistry* 48, 1123–1134.
- [9] Mueller, U. et al. (2012) Facilities for macromolecular crystallography at the Helmholtz-Zentrum Berlin. *J. Synchrotron Radiat.* 19, 442–449.
- [10] Kabsch, W. (2010) XDS. *Acta Crystallogr. D Biol. Crystallogr.* 66, 125–132.
- [11] CCP4 (1994) The CCP4 (Collaborative Computational Project Number 4) suite: programmes for protein crystallography. *Acta Crystallogr. D40*, 760–763.
- [12] Murshudov, G.N., Vagin, A.A. and Dodson, E.J. (1997) Refinement of macromolecular structures by the maximum-likelihood method. *Acta Crystallogr. D Biol. Crystallogr.* 53, 240–255.
- [13] Emsley, P. and Cowtan, K. (2004) Coot: model-building tools for molecular graphics. *Acta Crystallogr. D Biol. Crystallogr.* 60, 2126–2132.
- [14] Dean, A.M. and Dvorak, L. (1995) The role of glutamate 87 in the kinetic mechanism of *Thermus thermophilus* isopropylmalate dehydrogenase. *Protein Sci.* 4, 2156–2167.
- [15] Konarev, P.V., Volkov, V.V., Sokolova, A.V., Koch, M.H.J. and Svergun, D.I. (2003) PRIMUS: a Windows PC-based system for small-angle scattering data analysis. *J. Appl. Crystallogr.* 36, 1277–1282.
- [16] Guinier, A. (1939) La diffraction des rayons X aux très petits angles; application à l'étude de phénomènes ultramicroscopiques. *Ann. Phys.* 12, 166–237.
- [17] Svergun, D.I. (1992) Determination of the regularisation parameter in indirect-transform methods using perceptual criteria. *J. Appl. Crystallogr.* 25, 495–503.
- [18] Svergun, D.I., Barberato, C. and Koch, M.H.J. (1995) CRY SOL – a program to evaluate X-ray solution scattering of biological macromolecules from atomic coordinates. *J. Appl. Crystallogr.* 28, 768–773.
- [19] Gráczer, É., Konarev, P.V., Szimler, T., Bacsó, A., Bodonyi, A., Svergun, D.I., Závodszy, P. and Vas, M. (2011) Essential role of the metal-ion in the IPM-assisted domain closure of 3-isopropylmalate dehydrogenase. *FEBS Lett.* 585, 3297–3302.
- [20] Weiss, M.S. (2001) Global indicators of X-ray data quality. *J. Appl. Cryst.* 34, 130–135.